


Sound attenuation in air–water media with rough bubbly interface at low frequencies considering bubble resonance dispersion

Alireza Bolghasi¹ · Parviz Ghadimi¹  · Mohammad A. Feizi Chekab¹

Received: 24 December 2016 / Accepted: 6 July 2017 / Published online: 13 July 2017
© The Brazilian Society of Mechanical Sciences and Engineering 2017

Abstract The importance of incorporating the surface bubbles in acoustic modeling lies in the significant effects of the bubbly layer of the sea surface on the sound scattering, attenuation, and reflection. In the present paper, an acoustical system consisting of water, air, and bubbly water is considered and a particular approach incorporating a new version of the power-law concept for volumetric and scattering attenuation of bubbles is presented for the prediction of low-frequency damping of the sound in near-surface propagation. Sound attenuation in this system is traced in four steps and each step is considered as an individual case. Through applying the new power-law attenuation, the corresponding damping coefficient is derived. It has been shown by comparing the obtained results with experimental data that, at lower frequencies, the present model has better agreement with experiments than the theoretical model. Furthermore, a parametric study is conducted on different volume fractions and surface roughness, from which the equivalent damping coefficient of the free surface region is extracted using a mechanical and acoustical analogy to model the sound attenuation due to impedance difference, rough interface, bubbly water, and propagation range. It has been demonstrated that the present model can be used as an effective simple method for predicting the attenuation of sound in bubbly media with different bubble sizes.

Keywords Sound attenuation · Power-law attenuation · Bubble resonance dispersion · Damping coefficient · Acoustical system

1 Introduction

There are many different underwater sound sources such as underwater explosions, military training, marine vessels, active volcanoes, among others. Grelowska et al. [1] studied the main sources of acoustic waves related to marine vessels and different sources were identified at a low frequency ranging from 100 to 1000 Hz. It was concluded that generated noise in this spectral range is affected by the physical features of the propagation medium. The generated underwater noise propagates in various directions and hits different boundaries with particular properties. Accordingly, water–air interface occupying 2/3 of the earth’s surface has important implications in hydroacoustics [2]. As a result, it is quite natural that researchers would concentrate on the sound variation at water–air interface. Sea surface is studied from different point of views such as scattering, attenuation, and transmission of the incident sound. Hayat [3] developed a method for sound scattering near a penetrable plane which can be considered as a mathematical approach for the sea surface modeling. Sikora et al. [4], by focusing on ultrasounds, recently developed a beam tracing with refraction (BTR) method which simulates the reflection and refraction of sound in a medium. Although the goal of the majority of these studies has been the investigation of sound in the propagation medium, sound attenuation in the spectral region from 20 to 200 Hz remains largely an unexplored area in underwater acoustics [5]. However, various factors that are involved in sound attenuation cause major

Technical Editor: Kátia Lucchesi Cavalca Dedini.

✉ Parviz Ghadimi
pghadimi@aut.ac.ir

¹ Department of Marine Technology, Amirkabir University of Technology, Hafez Ave, No 424, P.O. Box 15875-4413, Tehran, Iran

difficulties in seeking an accurate solution. Influential factors such as the presence of waves, bubbles cloud, wind speed, and foam among others are some of the important factors. Understanding the effects of these factors and their originators is the complication of the next step. Tolstoy [6] presented an approach for calculating the damping coefficient of the interface of two different media with rough interface. By applying his relation and the known factors such as impedances of the two media, surface roughness parameter, and sound frequency, it is possible to calculate the sound damping factor.

In the real ocean surface, the generated sub-surface bubbles can significantly affect the incident sound to sea surface at low frequencies. Theory of sound propagation in fluid containing bubbles has been studied by different acousticians including Medwin [7], Hall [8], McDonald [9], Henyey [10], Prosperetti [11], Gauss and Fialkowski [12], Verestchagina and Fedotovskiy [13], Godin [14–16], Kuo [17], and White et al. [5]. For instance, Prosperetti [11] suggested the natural sound-producing mechanisms at frequencies between 20 and 500 Hz due to wave turbulence and oscillating bubble clouds. Medwin and Clay [18] examined the depth dependence of the bubbly layer on the attenuation of incident sound and concluded that it is a non-ignorable factor. Fialkowski and Gauss ([12] studied the important role of bubbles in surface scattering strength by decreasing the grazing angle and increasing the frequency and wind speed in the ocean. Verestchagina and Fedotovskiy [13] concluded that for sound propagation in the bubbly medium at low frequencies (below 200 Hz), the dynamic density of bubbly water medium should be taken into account due to the effects of bubbles dispersion. In the spectral region of 5–200 Hz, when the acoustic waves spread in a bubble medium due to progressive and volumetric deformation oscillations, the phase sound velocity is obtained using the effective dynamic density and effective dynamic compressibility of the medium [13]. This implies that impedance of the medium is different from the physical properties. Verestchagina and Fedotovskiy [19] derived a mathematical model for the resonance dispersion of the sound in gas–liquid media which showed good agreement with the experimental data. By applying their theory, it is possible to obtain the resonance-dependent phase velocity and sound damping factor in bubbly water medium at low frequencies. Despite the extensive applications of sound attenuation, not only in underwater sound propagation but also in the areas of biological studies like that reported by Klimonda [20], research on sound attenuation especially at low-frequency range has not been developed enough to fulfill the industrial and medical requirements. In underwater acoustics, almost all of the studies have concentrated on one or two effective parameters. Therefore, one can conclude that sound attenuation phenomenon at low

frequencies suffers from the lack of a comprehensive study which may include essential factors of sound attenuation in water and particularly near the air–water interface.

The main contribution of the present study is the presentation of a new version of the power-law attenuation for volumetric and scattering attenuation taking into account an acoustical system consisting of water, air, and bubbly water medium. In addition, a clear and comprehensive explanation of the free surface damping calculation, taking into account the bubble deformations and oscillations is provided to facilitate the reproduction of the model for the scientific community. Furthermore, the presented mathematical and parametric results in this study may have a wide range of applications in underwater communication channels, acoustic Doppler current profiler (ADCP), sonar performance, marine life, oceanography among others. For instance, in underwater communication channels, it is vital to know the effect of underwater boundaries such as sea surface on the signals to process the received signals and filter their noises. On the other hand, to send an appropriate signal securely in the media while it is capable of retaining the given information, it is crucial to have a clear view of sound attenuation in the propagation media. Therefore, knowing how sound is attenuated at the sea surface can significantly help acousticians in their studies. Accordingly, the aim of the current study is to present a particular mathematical model for studying the sound attenuation in water and air–water rough bubbly interface to approach a more realistic ocean condition. Therefore, to examine the sound attenuation in the spectral region of 5–200 Hz, a new version of power-law attenuation relation which considers both volumetric and scattering attenuations is derived. Subsequently, it is applied in an ocean-like acoustical system, where bubbles with the same radii are distributed in water to obtain the damping coefficient of the considered acoustical system.

2 Damping coefficient of two media with rough interface

If an acoustic medium is considered (as shown in Fig. 1) that occupies volume V (bounded by the boundary S) in which sound speed and density are, respectively, c and ρ , the wave equation for the acoustic pressure $p(\mathbf{x}, t)$ in such a medium, is described by

$$\rho \frac{\partial}{\partial x} \left(\frac{1}{\rho} \frac{\partial p}{\partial x} \right) + \rho \frac{\partial}{\partial y} \left(\frac{1}{\rho} \frac{\partial p}{\partial y} \right) + \rho \frac{\partial}{\partial z} \left(\frac{1}{\rho} \frac{\partial p}{\partial z} \right) - \alpha \frac{\partial p}{\partial t} - \frac{1}{c^2} \frac{\partial^2 p}{\partial t^2} + U(Q) \delta(\mathbf{x} - \mathbf{x}_s) = 0, \quad (1)$$

where α is the damping coefficient of the medium, t is time, while x , y , and z are the principal directions, \mathbf{x} is the

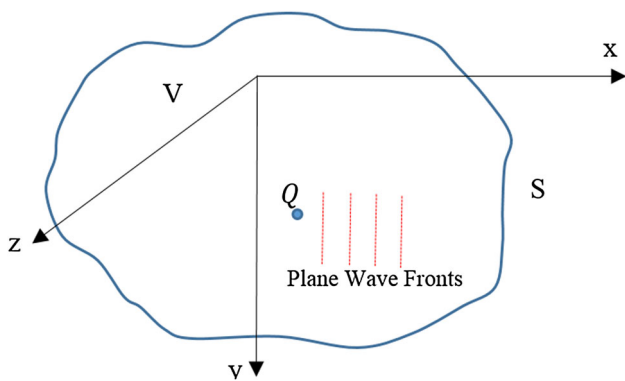


Fig. 1 Acoustic medium occupying volume V bounded by surface S [21]

propagation vector of the generated sound by the source Q , $U(Q)$ is the source strength, and x_s is the vector of the source position.

If volume V in Fig. 1 is considered to have the same boundary as the second medium V_2 with different impedance ($\rho_2 c_2$), as shown in Fig. 2, through a mathematical process, it is possible to derive the damping coefficient α for the propagation media of Fig. 2 as follows:

$$\alpha = \alpha_{SV} = \frac{\ln P_2 - \ln P_1}{(T - R)x} = \frac{\ln P_B - \ln P_D}{(T - R)x}, \tag{2}$$

where α_{SV} is the damping coefficient due to the scattering and volumetric attenuations, P_1 or P_D is the acoustic pressure arriving at the interface of the two media and P_2 or P_B is the boundary wave at the interface, and x is the total propagation range. In addition, T and R are the transmission and reflection coefficients. Equation (2) may be considered as a new version of power-law attenuation in which volumetric and scattering attenuations are involved. On the other hand, previous investigators including Szabo [22, 23] and Chen [24] have proposed a relation to obtain damping coefficient of a homogeneous medium as follows:

$$\alpha_V = \frac{\ln P_2 - \ln P_1}{x}, \tag{3}$$

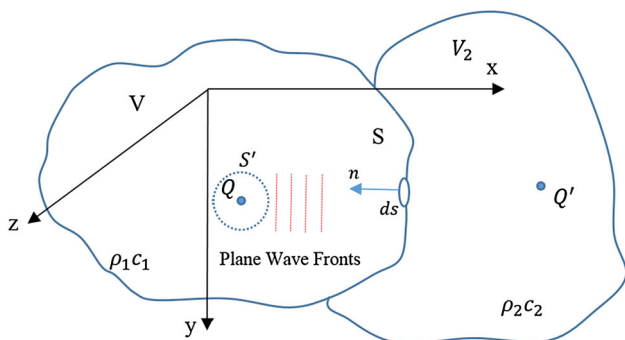


Fig. 2 Propagation of wave in media containing two different impedances with rough interface

where α_V is the damping coefficient due to only volumetric attenuation and x is the propagation range. Tolstoy [6] proposed a relation to calculate the damping factor due to the presence of a rough interface between two media with different impedances. Through his proposed relation, it is possible to calculate the scattering attenuation for an acoustic wave, when it passes the rough boundary of two media. His derived relation is

$$\alpha_{Tol} = \frac{1}{2N} \frac{g_1 (\beta^2 + 0.5\alpha_0^2) k_1^3}{\left(1 + \frac{\rho_1 g_1}{\rho_2 g_2}\right)}, \tag{4}$$

where α_{Tol} is Tolstoy’s damping coefficient for the rough interface of the two media. Other variables in Eq. (4) are defined as

$$g_i = \left(k^2 - \frac{\omega^2}{c_i^2}\right)^{0.5}, \tag{5a}$$

$$\alpha_0 = \tau(1 + \mathcal{K}) \left(1 - \rho_1/\rho_2\right), \tag{5b}$$

$$\tau = 0.5NV_0, \tag{5c}$$

$$\beta = \tau \left(1 - m_1/m_2\right), \tag{5d}$$

where k is the acoustic wave number, c_i is the sound velocity of each medium, and ω is the circular frequency. Additional variables are defined in Table 1.

3 Acoustical system of air–water media with rough bubbly interface

In the real sea states, mostly sub-surface bubbles are generated as a result of different phenomena such as breaking waves, moving floating objects, rainfall, etc. The bubbles cloud under air–water interface can cause significant effects on the incident sound features. These effects at frequencies below 200 Hz are more important when resonance dispersion of the incident sound occurs. In addition, due to the resulting dynamic density and

Table 1 Definition of some parameters in Tolstoy’s damping relation

| Parameter | Definition |
|--|--|
| \mathcal{K} | Virtual mass coefficient of the full scatterer |
| m_1/m_2 | Ratio of compressibilities of the two media |
| V_0 | Full scatterer volume |
| h | Correlation distance for a random surface |
| $N = \frac{1}{h^2} \sqrt{\frac{1}{2.3}}$ | Number of scatterers per unit area |
| $m = \frac{1}{\rho c^2}$ | Isentropic compressibility |
| $c^2 = \frac{\partial p}{\partial \rho}$ | Sound speed in classical mechanics |

phase velocity, the impedance of the medium can be different from an ordinary one without the dispersion effects. Therefore, the sub-surface layer of bubbles is considered as an extra third medium (in addition to air and water) having its own features. In the current study, bubbly layer sandwiched between air and water media is considered to have homogenous property in sizes of bubbles. Although in reality bubbles vary in their sizes and distributions, to simplify the modeling, it is possible to consider a dominant radius for the bubbles in the bubbly water medium [18]. However, in an ideal case, it would be more physically appropriate to consider the 3D spatial distribution of bubbles and wide distribution of sizes. In the current study, the bubble’s radius is considered to be 1 mm. In addition, the air and water densities are considered to be 1.2 kg/m³ and 1020 kg/m³, respectively. The speed of sound in air and water are considered to be 340 and 1500 m/s, respectively.

To simulate the physical phenomenon of sound attenuation due to rough bubbly water interface more realistically, an acoustical system is considered which is shown in Fig. 3. In the present modeling, the considered acoustical system is excited by a localized point source in the water which emits a ping towards rough bubbly air–water interface. The emitted ping will be damped in the acoustical system due to the impedance differences between the three media of air–water–rough interface and resonance dispersion in the bubbly medium. Therefore, to examine the damping phenomenon in the considered acoustical system, the emitted ping is followed in the media through four different sequences. These sequences are displayed in Fig. 4. Traveling the distance x in the water, the initial ping with pressure P_{inc1} will face the imaginary interface of water–bubbly water in its first sequence, as shown in Fig. 4a. Volumetric and scattering attenuation will be the results of this step. Impedance difference between two media causes transmission and scattering of the remaining ping pressure. In the second step, transmitted pressure P_{inc2} is volumetrically

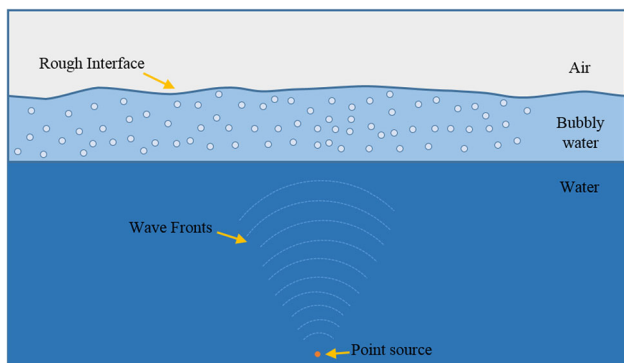


Fig. 3 Schematic of the simulation

attenuated while passing the bubbly water medium (Fig. 4b). Finally, the part of the pressure which strikes the air–bubbly water interface simultaneously experiences two different damping phenomena. It is attenuated due to the rough interface and the impedance differences between air and bubbly water media. To examine the attenuation practically, this sequence is divided into two different steps which are shown in Fig. 4c, d.

By eliminating the source singularity at the distance R , where $\lambda \ll R$, it is possible to consider the emitted spherical wave as a plane wave in the acoustical system. Therefore, plane wave relations can be used in the rough bubbly surface region within the acoustical system. Applying the following equation, Brekhovskikh et al. [25] expanded the generated spherical wave ($R^{-1} \exp(ikR)$) into plane wave:

$$P_i = \frac{\exp(ikR)}{R} = i(2\pi)^{-1} \iint_{-\infty}^{\infty} k_z^{-1} \exp[i(k_x x + k_y y + k_z z)] dk_x dk_y. \quad (6)$$

For the converted plane wave Eq. (6), the reflected and transmitted waves can be obtained, respectively, as follows:

$$P_r = i(2\pi)^{-1} \iint_{-\infty}^{\infty} k_{1z}^{-1} \mathcal{R}(k_{1z}) \exp[i(k_{1x} x + k_{1y} y + k_{1z}(z + z_0))] dk_{1x} dk_{1y}, \quad (7)$$

$$P_t = i(2\pi)^{-1} \iint_{-\infty}^{\infty} k_{2z}^{-1} \mathcal{T}(k_{2z}) \exp[i(k_{2x} x + k_{2y} y + k_{2z}(z + z_0))] dk_{2x} dk_{2y}, \quad (8)$$

where k_1 and k_2 and their components are wave numbers in medium V and medium V_1 , and \mathcal{R} is the reflection coefficient.

Evaluating the integrals in Eqs. (7) and (8), the reflected and transmitted pressure fields within the acoustical system can be obtained as in [25]

$$P_r = \mathcal{R}(\theta_1) R_1^{-1} \exp(ikR_1), \quad (9)$$

$$P_t = \mathcal{T}(\theta_1) R_2^{-1} \exp(ikR_2), \quad (10)$$

where θ_1 is the incidence angle, $\mathcal{R}(\theta_1)$ is the reflection coefficient, $\mathcal{T}(\theta_1)$ is the transmission coefficient, and R_1 and R_2 are, respectively, Q and Q' distances away from the struck element (ds) on the boundary S (Fig. 2). Applying the theory of plane wave, the reflection and transmission coefficients can be derived as

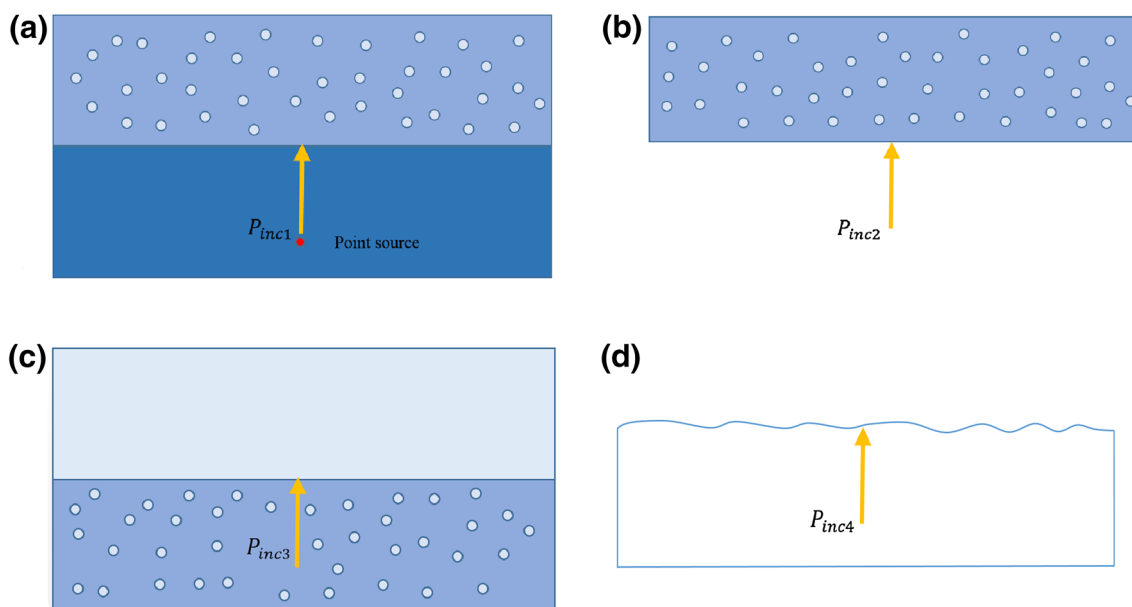


Fig. 4 Four different sequences in damping phenomenon: **a** Incident ping P_{inc1} is emitted to water and bubbly water interface, **b** transmitted pressure of the first sequence P_{inc2} passes the bubbly

water medium. Remaining pressure of the last sequences strikes, **c** bubbly water and air interface by P_{inc3} , and **d** rough surface by P_{inc4}

$$\mathcal{R} = \frac{m' \cos \theta_1 - n' \cos \theta_2}{m' \cos \theta_1 + n' \cos \theta_2} = \frac{m' \cos \theta_1 - \sqrt{n'^2 - \sin^2 \theta_1}}{m' \cos \theta_1 + \sqrt{n'^2 - \sin^2 \theta_1}}, \tag{11}$$

$$\mathcal{T} = \frac{2m' \cos \theta_1}{m' \cos \theta_1 + \sqrt{n'^2 - \sin^2 \theta_1}}, \tag{12}$$

where θ_2 is the inclination angle in the medium V_1 , and n' and m' are defined as follows:

$$n' = \frac{k_1}{k_2} = \frac{c_2}{c_1}, \tag{13a}$$

$$m' = \frac{\rho_2}{\rho_1}. \tag{13b}$$

In the following subsections, the emitted ping will be followed in the acoustical system in four sequences, as shown in Fig. 4, and damping coefficient of each sequence will be derived.

3.1 Damping coefficient of case (a)

In this case, the incident ping generated by a point source is emitted towards the interface of water and bubbly water (Fig. 4a). Considering the propagation range from the source location to the element ds (in Fig. 2), the incident pressure P_{inc1} and its scattering from the interface of the two media, P_{r1} , are, respectively, the acoustic arrival P_D and boundary wave P_B for the current case. By substituting Eqs. (6) and (9) as arriving and boundary waves in Eq. (2),

the damping coefficient of case (a) labeled as α_{SVa} can be obtained as follows:

$$\alpha_{SVa} = \frac{\ln P_B - \ln P_D}{(\mathcal{T} - \mathcal{R})x_a} = \frac{\ln P_{r1} - \ln P_{inc1}}{(\mathcal{T}_a - \mathcal{R}_a)x_a} = \frac{1}{(\mathcal{T}_a - \mathcal{R}_a)x_a} \times \ln \frac{\mathcal{R}_a R_{r1}^{-1} \exp(ik_1 R_{r1})}{R_1^{-1} \exp(ik_1 R_1)}, \tag{14}$$

where \mathcal{R}_a and \mathcal{T}_a are reflection and transmission coefficients of case (a), R_1 is the propagation range of the arriving wave, R_{r1} is the propagation range of the boundary wave, and $x_a = R_{r1} + R_1$ is the total distance traveled by both waves in medium V (Fig. 2). Equation (14) can be rewritten as

$$(\mathcal{T}_a - \mathcal{R}_a)x_a \alpha_{SVa} = \ln \frac{\mathcal{R}_a R_1}{R_{r1}} + ik_1(R_{r1} - R_1). \tag{15}$$

Since the left-hand side of Eq. (15) is real, the imaginary component on the right-hand side of the equation should be zero. As a result, the damping coefficient of the case (a) is as follows:

$$\alpha_{SVa} = \Re \left(\frac{1}{(\mathcal{T}_a - \mathcal{R}_a)x_a} \times \left[\ln \left(\frac{\mathcal{R}_a R_1}{R_{r1}} \right) + ik_1(R_{r1} - R_1) \right] \right). \tag{16}$$

3.2 Damping coefficient of case (b)

In this case, the damping factor of the bubbly water itself is targeted. As pointed out earlier, based on the resonance

dispersion model (RDM) at low frequencies, bubble deformation can play a major role in damping of the entering sound. Furthermore, it causes dynamic density of the medium and phase velocity of the passing sound. Although the resonance dispersion of bubbly water is targeted in this paper, both simple non-deformed bubbles and RDM in bubbly water medium are examined for comparison purposes. In the current case [i.e., case (b)], by applying RDM model, the dynamic density, sound phase velocity, and damping coefficient of the medium are obtained via the following relations [19]:

$$\rho_{bw}^* = \rho_w \left(\frac{\rho^*}{\rho} \right)_0 + \frac{\phi}{\gamma_0} \left(\frac{A'}{a} \right)^2 \frac{(2\omega/\omega_2)^2}{1 - (2\omega/\omega_2)^2}, \tag{17}$$

$$\left(\frac{\rho^*}{\rho} \right)_0 = (1 - \phi)/(1 + 2\phi), \tag{18a}$$

$$\gamma_0 = \frac{1 + 2\phi}{2(1 - \phi)}, \tag{18b}$$

$$\beta^* = \frac{1 - \phi}{\rho_w C_w^2} + \frac{\phi}{\rho_a C_a^2}, \tag{18c}$$

$$C^* = \frac{1}{\sqrt{\beta^* \rho_{bw}^*}}, \tag{18d}$$

where ρ_{bw}^* is the dynamic density of bubbly water medium, a is the bubble radius, C_w and C_a are, respectively, the speed of sound in water and air, ρ_w and ρ_a are, respectively, water and air densities, γ_0 is the added mass parameter for the spherical bubbles, ϕ is the void fraction, β^* is the effective compressibility, C^* is the RDM sound velocity, $\omega = 2\pi f$ (where f is sound frequency) is the angular frequency of sound, ω_2 is the natural angular frequency of the spheroid oscillations of bubble [26] which is determined by $\omega_2 = \sqrt{12\tau/\rho_w a^3}$, where τ is the surface tension. For the considered conditions of $\rho_w = 1020 \text{ kg/m}^3$, $a = 0.001 \text{ m}$, $\tau = 0.074 \text{ N/m}$.

In the current study, ω_2 is taken to be 933 rad/s. In addition, $A' = U_0/\omega$ is the amplitude of medium oscillations, and as discussed and derived by Verestchagina and Fedotovskiy [19], U_0 is the oscillation velocity of the medium (which is hereby water). Verestchagina and Fedotovskiy [19] stated that the first term of Eq. (17) represents the dynamic density of the medium with spherical bubbles, and the second term represents the effect of resonance dependence of dynamic density at frequencies close to half of the natural frequency of the oscillation of bubbles. Damping coefficient of the bubbly water medium which is the damping coefficient in case (b), can be obtained as follows [19]:

$$\alpha_b = \frac{\eta^*}{2} \sqrt{\frac{\beta^*}{\rho_{bw}^*}} + \frac{\omega^2}{\omega_0} \beta_1 \rho_w C_w \phi \xi, \tag{19}$$

where ω_0 is the natural angular frequency of the volumetric oscillations of bubbles [18] which can be calculated based on the radius and depth of the bubble (for instance, its value is around 3.25 kHz). In addition, β_1 is the polytropic compressibility of gas in bubbles, which calculation was discussed by Minnaert [27], Nakoryakov et al. [28], and Skudzuk [29]. It should be pointed out that higher modes of oscillation have much lower impact on the damping of sound in low frequencies and, therefore, have not been incorporated in the formulation. In addition, detailed procedure for obtaining the translation velocity η^* was presented by Verestchagina and Fedotovskiy [19]. In addition, parameter ξ in Eq. (19) consists of two items as follows:

$$\zeta_s = \frac{\rho \omega^3 a^3}{3\kappa P_0 C} = \frac{\rho(\omega_0 a)^3}{3C_w \rho_a C_a^2} \left(\frac{\omega}{\omega_0} \right)^3, \tag{20}$$

$$\zeta_{th} = \frac{3(\kappa - 1)}{a\sqrt{2\omega/\chi}}, \tag{21}$$

where κ and χ are the thermal conductivity and index of polytropic of gas in the bubbles, respectively. Both ζ_s and ζ_{th} can be obtained as discussed by Verestchagina and Fedotovskiy [19]. It should be mentioned that the volumetric resonance does not significantly affect the phase velocity in Eq. (18d) due to the fact that phase velocity depends on the dynamic density of the bubbly water medium and the effective compressibility. The volumetric resonance affects these two parameters in time. However, the current analysis is not relevantly close to volumetric resonance frequencies.

Individually and independent of the considered sequences in the acoustical system, damping coefficient for this case is obtained. However, it is necessary to discuss the input and output acoustic pressures of the bubbly water medium to follow the third and fourth sequences of the considered acoustical system. When the arriving wave $P_D = P_{inc1}$ in case (a) hits the water–bubbly water interface, it is transmitted to the next medium, while part of its energy is attenuated due to the damping of case (a). In addition, the boundary wave in case (a) can be obtained as follows:

$$\alpha_{SVa} = \frac{\ln P_B - \ln P_D}{(\mathcal{T}_a - \mathcal{R}_a)x_a} = \frac{\ln P_B - \ln P_{inc1}}{(\mathcal{T}_a - \mathcal{R}_a)x_a} \rightarrow P_B = e^{(\mathcal{T}_a - \mathcal{R}_a)x_a \alpha_{SVa}} P_{inc1}. \tag{22}$$

Therefore, part of the boundary wave which is transmitted to the bubbly water medium is obtained as

$$P_{inc2} = \mathcal{T}_a P_B = \mathcal{T}_a e^{(\mathcal{T}_a - \mathcal{R}_a)x_a \alpha_{SVa}} P_{inc1} = \frac{\mathcal{T}_a}{R_1} \exp[(ik_1 R_1 + (\mathcal{T}_a - \mathcal{R}_a)x_a \alpha_{SVa})]. \tag{23}$$

Hence, through Eq. (23), the arriving wave to the bubbly medium can be obtained. The computed damping

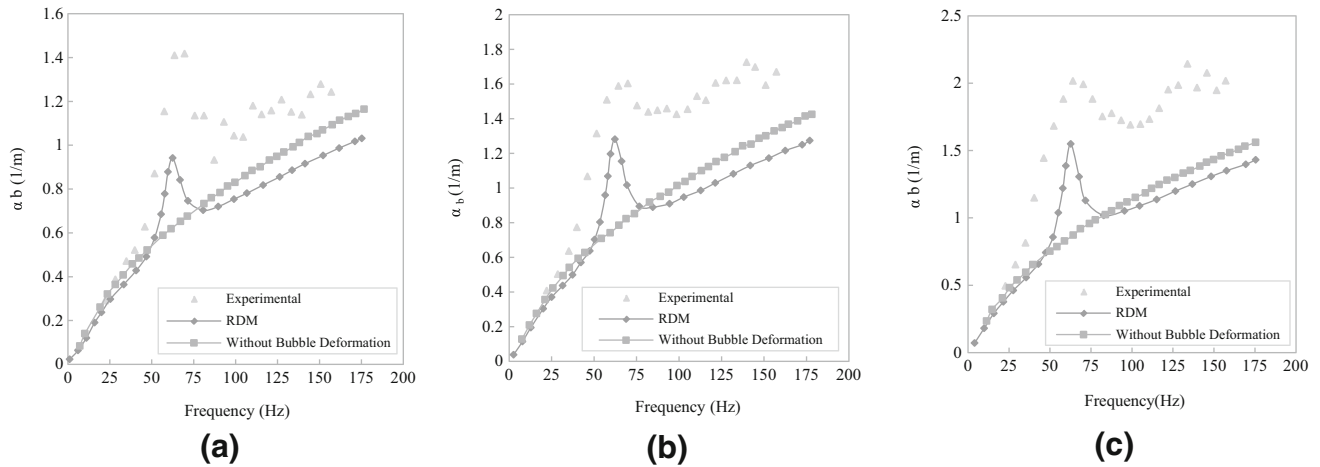


Fig. 5 Damping coefficients of sound in bubbly water medium: **a** $\Phi = 0.08$, **b** $\Phi = 0.12$, **c** $\Phi = 0.15$ [19]

coefficient for case (b) in different volume fractions is displayed in Fig. 5.

3.3 Damping coefficient of case (c)

In this case, the transmitted pressure of case (a) to the bubbly water medium propagates within bubbly water with a new angle (θ_1) which is caused by the difference in the impedances. For the same reason, the wave number is changed and it is labeled as k_2 . In addition, since the arriving pressure P_{inc2} , while passing through the bubbly medium, is damped due to the bubble presence, whether according to RDM or non-dispersion models, it is suggested that P_{inc2} is multiplied by e^{α_b} to eliminate the interactions of all cases. Practically, cases (c) and (d) occur, simultaneously. Therefore, the same arriving pressures for these cases are considered as

$$P_{inc3} = P_{inc4} = e^{\alpha_b} P_{inc2} = \frac{T_a}{R_1} \exp[ik_1 R_1 + (T_a - \mathcal{R}_a)x_a \alpha_{SVa} + \alpha_b]. \tag{24}$$

On the other hand, since the impedance difference and rough surface in cases (c) and (d) are the causes of damping phenomenon, boundary waves of these cases will be different. Therefore, P_{rc} and P_{rd} which are, respectively, boundary waves in case (c) as a result of impedance difference and in case (d) as a result of rough interface, are individually obtained. Therefore, P_{rc} for the boundary wave of the current case is

$$P_{rc} = \mathcal{R}_c(\theta_1) \exp(ik_1 R_3), \tag{25}$$

where $\mathcal{R}_c(\theta_1)$ is the reflection coefficient of case (c) which is the result of the impedance differences between air and bubbly water media, and R_3 is the propagation range of the boundary wave P_{rc} . Applying Eq. (25), the damping coefficient of case (c) can be computed as follows:

$$\begin{aligned} \alpha_{SVc} &= \frac{1}{(T_c(\theta_1) - \mathcal{R}_c(\theta_1))x_c} \times \ln \frac{P_{rc}}{P_{inc3}} \\ &= \frac{1}{(T_c(\theta_1) - \mathcal{R}_c(\theta_1))x_c} \times \ln \frac{R_1 \mathcal{R}_c(\theta_1) \exp(ik_1 R_3)}{T_a R_3 \exp[ik_1 R_1 + (T_a - \mathcal{R}_a)x_a \alpha_{SVa} + \alpha_b]}, \end{aligned} \tag{26}$$

where x_c is the propagation distance in case (c). By considering the real part of Eq. (26), α_{SVc} can be obtained as follows:

$$\begin{aligned} \alpha_{SVc} &= \Re \left(\frac{1}{(T_c(\theta_1) - \mathcal{R}_c(\theta_1))x_c} \times \left[\ln \left(\frac{R_1 \mathcal{R}_c(\theta_1)}{R_3 T_a} \right) \right. \right. \\ &\quad \left. \left. - (T_a - \mathcal{R}_a)x_a \alpha_{SVa} + \alpha_b + ik_1 \left(R_3 - \frac{1}{R_1} \right) \right] \right). \end{aligned} \tag{27}$$

3.4 Damping coefficient of case (d)

In this case, effects of rough surface on the arriving sound are targeted. As pointed out earlier, the arriving wave is the transmitted sound of case (a) multiplied by e^{α_b} . In addition, boundary wave P_{rd} can be calculated through reflection coefficient of small perturbation method (SPM) as follows:

$$\mathcal{R}_d = \mathcal{R}_{pert} = 1 - 7.682 \times 10^{-5} \left(f^{3/2} h_{rms}^{8/5} \Gamma \right). \tag{28}$$

Here, $\mathcal{R}_d = \mathcal{R}_{pert}$ is the reflection coefficient of case (d), f is the sound frequency, h_{rms} is the rms of the wave height, and $\Gamma = \cos \theta_1$ is the polar angle of the arriving wave direction. In the proposed approach, h_{rms} is equal to the correlation distance for a random surface (h) defined by Tolstoy [6]. Therefore, for the boundary wave P_{rd} , the following relation can be assumed:

$$P_{rd} = R_4^{-1}(\mathcal{R}_d) \exp(ik_1 R_4), \tag{29}$$

where R_4 is the propagation range of boundary wave P_{rd} . Therefore, by applying Eq. (2), the damping factor of the present case can be obtained as follows:

$$\begin{aligned} \alpha_{SVd} &= \frac{1}{(\mathcal{T}_d(\theta_1) - \mathcal{R}_d(\theta_1))x_d} \times \ln \frac{P_{rd}}{P_{inc4}} \\ &= \frac{1}{(\mathcal{T}_d(\theta_1) - \mathcal{R}_d(\theta_1))x_d} \\ &\quad \times \ln \frac{R_1(\mathcal{R}_d) \exp(ik_1 R_4)}{\mathcal{T}_a R_4 \exp[ik_1 R_1 + (\mathcal{T}_a - \mathcal{R}_a)x_a \alpha_{SVa} + \alpha_b]}, \end{aligned} \tag{30}$$

where x_d is the total propagation range of case (d) and $\mathcal{T}_d(\theta_1)$ is the transmission coefficient of case (d). It is now possible to compute the damping coefficient of each case through the derived relations. In the following section, the effects of different parameters involved in damping phenomenon within the acoustical system will be discussed.

4 Parametric study

To apply the derived relations in the previous sections, an acoustical system which is a representation of a real sea condition consisting of water, bubbly water, and air media is selected. However, for simplification purposes, the dominant bubbles of 1 mm radius are considered to be distributed in the bubbly medium. In this acoustical system, a localized point source which emits a ping towards the sea surface region causes an excitement in the environment. As outlined earlier, the derived relations can be applied to the range $\lambda \ll R$. In this paper, propagation at low frequencies ($5 \text{ Hz} < f < 200 \text{ Hz}$) is investigated and by considering the speed of sound in water as 1500 m/s, λ

is varied from 7.5 to 300 m. Therefore, to satisfy the range condition, a mean value $R_1 = 1000 \text{ m}$ in water is considered for all frequencies. A mean value for all frequencies is considered to study the sound damping coefficient in the same source condition and omit its influence on the damping coefficient. For the current acoustical system, the damping variations of case (a) with respect to the frequency and in three different volume fractions are displayed in Fig. 6. As evident in this figure, results of the resonance dispersion are different from those of the non-resonance dispersion model. Equation (22) is applied to calculate the damping coefficient of case (a) in two different conditions: (1) considering the resonance dispersion and (2) not considering the resonance dispersion. To verify the accuracy of the damping values in all volume fractions, the obtained results are compared to that of Tolstoy’s approach. Furthermore, according to Eq. (22) and the RDM model, due to sudden fall in sound velocity around 50 Hz frequency, the value of the damping coefficient increases abruptly. Verestchagina and Fedotovskiy [19] mentioned that resonance dispersion of the sound for bubbly medium takes place at a frequency of about 50–60 Hz. In this frequency range, resonance dispersion of the sound and resonance damping occur due to the increase of progressive oscillations amplitude of bubbles and also the increase of viscous losses at resonance of deformation–progressive oscillations of bubbles. Consequently, the peak of the damping results in the frequency range 50–60 Hz, as seen in Fig. 6, seems reasonable. In addition, based on the RDM, the resulting damping coefficients of the dispersion state are hereby higher than those of non-dispersion state due to phase velocity of the sound and dynamic density of the bubbly medium. In Fig. 6, it can be seen that the results of Tolstoy’s approach are generally less than those of the considered approach in

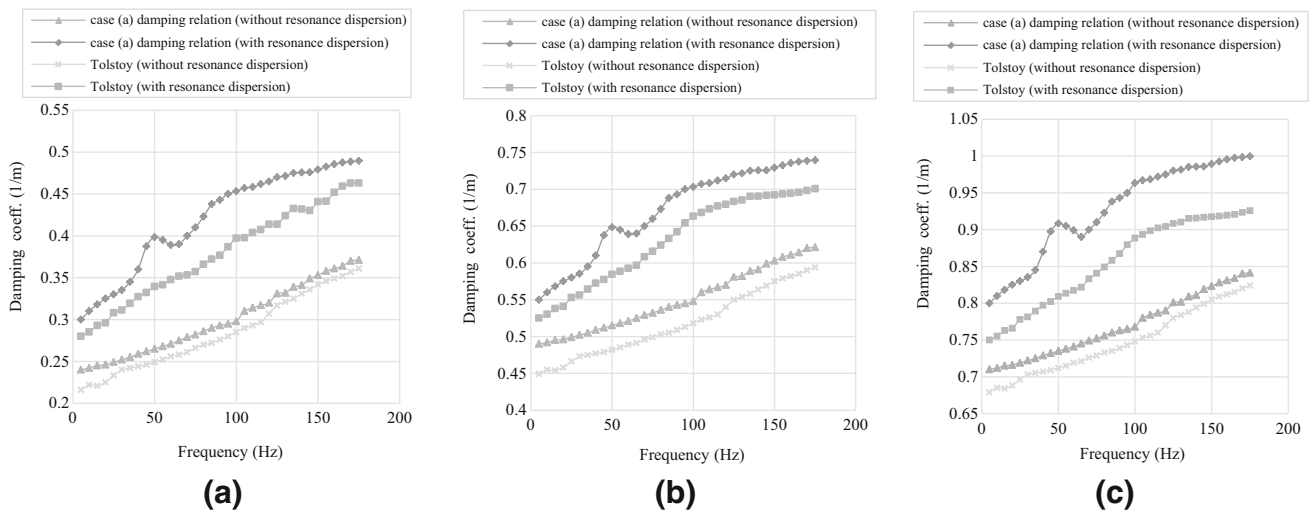
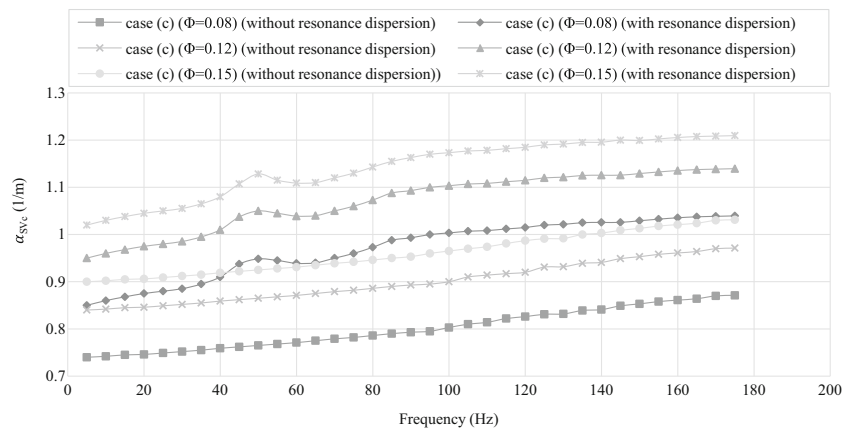


Fig. 6 Damping coefficients in case (a): a $\Phi = 0.08$, b $\Phi = 0.12$, c $\Phi = 0.15$

Fig. 7 Damping coefficients in case (c) using the corresponding derived relation



the current study, and also do not show the peaked damping in the frequency range of 50–60 Hz. This might be due to ignoring the viscous losses in the Tolstoy’s approach [6] because, as mentioned, based on the RDM approach, the damping due to viscous losses at resonance of deformation–progressive oscillations of bubbles is one of the two reasons that increases the damping coefficients abruptly at frequency range 50–60 Hz.

In both resonance dispersion and non-resonance dispersion states, the Tolstoy’s approach [6] and the approach adopted in the current study depend on the physical features of the medium such as density of medium and sound velocity. However, the considered approach here also considers the attenuation due to the propagation range which is directly involved in the damping relations. Since in the Tolstoy’s approach [6], the propagation range is not involved, the resulting damping coefficients from Tolstoy’s approach are generally less than those of the current study which considers the propagation range as a variable which causes the attenuation.

Figure 7 illustrates the damping coefficient vs. the frequency for case (c). Equation (27) is taken into account to calculate the damping coefficients of case (c) for the resonance dispersion model and the none-resonance dispersion model. As volume fraction increases, a growth in the damping coefficients in both resonance dispersion and none resonance dispersion states is observed. In fact, in this case, at the same volume fractions, the damping coefficients of the resonance dispersion state are generally higher than those of the non-resonance dispersion case. Figure 8 depicts the results of damping coefficient for case (d). Since in this case, the surface roughness is an important variable in the variation of damping coefficients, studying its influence becomes necessary. Therefore, two different surface values of 0.75 and 1.5 m are considered for the surface roughness. As evident in Fig. 8, a growth in surface roughness causes an increase in damping coefficient which seems reasonable. This growth is seen in all volume fractions and in both resonance dispersion and non-resonance dispersion states. At the same surface roughness and

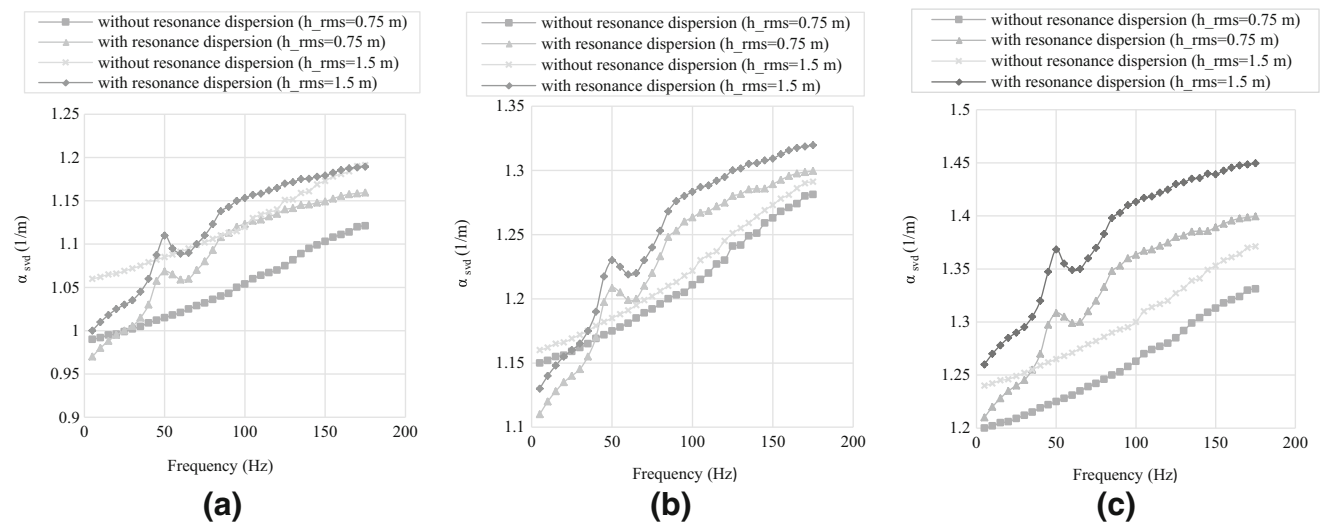


Fig. 8 Damping coefficients in case (d): **a** $\Phi = 0.08$, **b** $\Phi = 0.12$, **c** $\Phi = 0.15$

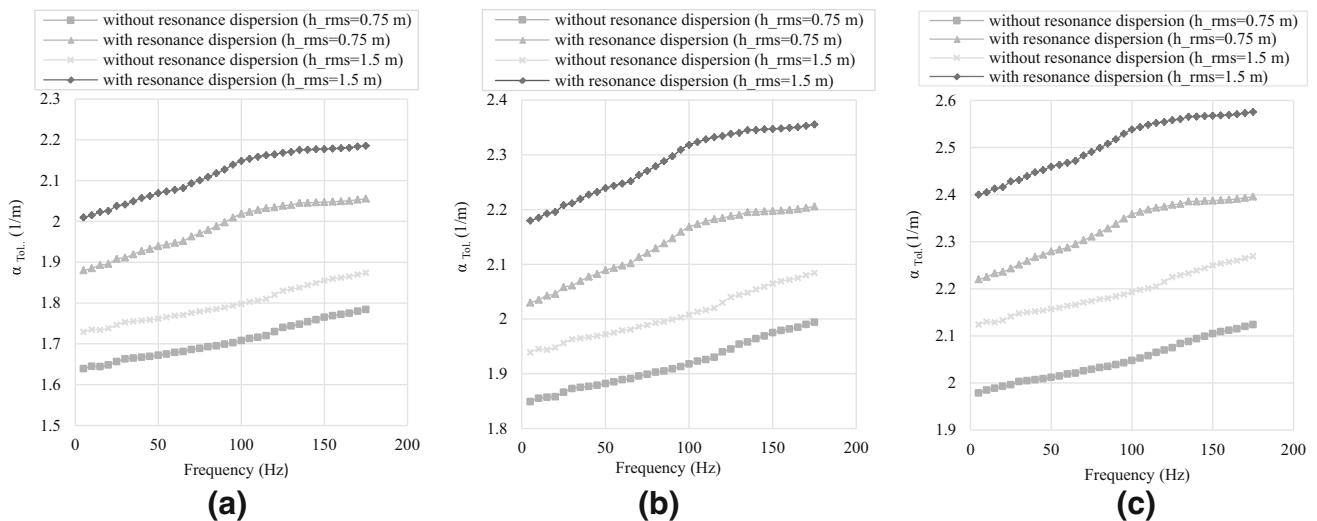


Fig. 9 Damping coefficients in cases (c) and (d) by Tolstoy's approach: **a** $\Phi = 0.08$, **b** $\Phi = 0.12$, **c** $\Phi = 0.15$

volume fraction and at frequencies higher than half of the natural frequency of the spheroid oscillations of bubbles (which is hereby between 50 and 60 Hz), the damping coefficients of the resonance dispersion state are higher than those of the non-resonance dispersion state. Below the mentioned frequency range, the damping coefficients of the non-dispersion state are higher than those of the dispersion state. These variations in the damping coefficients, as frequency varies, are related to the effect of the surface roughness. In fact, the reflection and transmission coefficients of case (d) are functions of the frequency and surface roughness, despite the reflection and transmission coefficients of the other cases, which are functions of sound speed and density of the medium. However, as volume fraction increases, the results of resonance dispersion state tend to overcome those of non-resonance dispersion state at all frequencies. This is related to the effects of bubbly medium (volumetric effects) which become more influential than the effects of surface roughness, as volume fraction increases.

Since cases (c) and (d) occur simultaneously, the results of Tolstoy's approach [6] for both cases can be utilized. Results are seen in Fig. 9. Indeed, it is possible through Tolstoy's approach [6] to calculate the damping coefficient of two media with rough interface. Therefore, it is not necessary to separate case (c) from case (d) in this approach. Figure 9 shows the results of Tolstoy's approach [6] for both dispersion and non-dispersion states in two different considered surface roughness. In addition, through his approach, growth in damping coefficients is observed as volume fraction and frequency increase.

As illustrated in Fig. 9a (for 0.08 volume fraction), at 100 Hz frequency and 1.5 m surface roughness, the value of damping coefficient is 2.15 (1/m). Through considering the resonance dispersion state, and the related damping

coefficients for 0.08 volume fraction and 100 Hz frequency in Fig. 7a, and also for 0.08 volume fraction, 1.5 m surface roughness, and 100 Hz frequency in Fig. 8a, it can be seen that the damping coefficients are 1 (1/m) and 1.15 (1/m) for cases (c) and (d), respectively. Therefore, the sum of these values of damping coefficients is equal to the one in the Tolstoy's approach [6]. Considering the same conditions, but for 0.15 volume fraction, the damping coefficients of case (c) (Fig. 7) and case (d) (Fig. 8) are 1.175 (1/m) and 1.415 (1/m), respectively. In the same conditions (1.5 m surface roughness, 0.15 volume fraction, and 100 Hz frequency), the damping coefficient of the Tolstoy's approach [which is, in fact, the result of combined cases of (c) and (d)] is 2.53. On the other hand, the sum of the two mentioned damping coefficients for 0.15 volume fraction is 2.58. Therefore, the final values are almost equal and the difference might be related to neglecting the viscosity in Tolstoy's approach, which is an important factor as volume fraction increases. Despite case (a), where the gap between the resulting values from the current scheme and Tolstoy's approach [6] is wider, here the differences may just be due to neglecting the viscous effects. In fact, since in case (a) the propagation range is a lot larger than that of combined cases of (c) and (d) and the Tolstoy's approach [6] neglects the role of propagation range, the accumulation error in Tolstoy's approach may occur where both propagation range and viscous effects are important.

5 Analogies between the acoustical and mechanical systems

In the previous section, the calculated damping coefficients of the acoustical system in four different cases were presented, and results were compared to those through

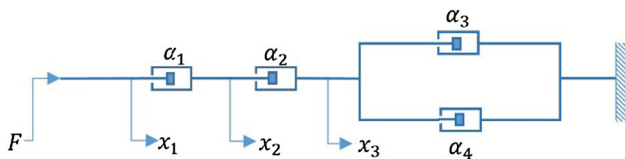


Fig. 10 Mechanical system excited by momentary exciting force F . x_1, x_2 , and x_3 are the system’s displacements

Tolstoy’s approach [6]. However, to compute the total damping coefficient of the system, analogies between the acoustical and mechanical systems are studied. For the mechanical system arrangement, the dampers are considered as illustrated in Fig. 10. In the considered acoustical system, sound attenuation due to the water and bubbly water interface is represented by α_1 in the mechanical system. In the next sequence, sound attenuation in a bubbly water medium is symbolized by α_2 in the mechanical system. These two sequences occur one after another and the dampers α_1 and α_2 are arranged in a series in the mechanical system. On the other hand, since cases (c) and (d) occur simultaneously, the dampers α_3 and α_4 in the mechanical system that represent air–bubbly water interface and surface roughness attenuations in the acoustical system are positioned in a parallel arrangement. As discussed in the previous section, this arrangement might be appropriate since the resulting equivalent damping coefficient for the combined cases of (c) and (d) showed good agreement with that of Tolstoy’s approach. Therefore, the considered acoustical system is identical to a mechanical system which is shown in Fig. 10.

If the mechanical system is excited by a sudden and momentary force F , the equivalent damping of the system can be obtained as

$$\alpha_{eq} = \frac{\alpha_1 \alpha_2}{\alpha_1 + \alpha_2} + (\alpha_3 + \alpha_4). \tag{31}$$

Through the analogies made between the acoustical and mechanical system, the total damping coefficient of the acoustical system is to be calculated using damping coefficients of the considered cases. Applying Eq. (31), the predicted equivalent damping coefficients of the acoustical system vs. frequency are shown in Figs. 11 and 12 for both surface roughness of 0.75 and 1.5 m. Figure 11 shows the difference between the damping coefficients for dispersion and non-dispersion states and the resulting damping coefficients in the resonance dispersion state are generally higher. Furthermore, in the damping curves of dispersion states, crests are seen in the spectral region of 50–70 Hz. This happens due to the sudden reduction of the sound speed in this spectral region [19]. These crests are quite visible in Fig. 12, too. In both roughness heights of 0.75 and 1.5 m, generally damping coefficients grow within the

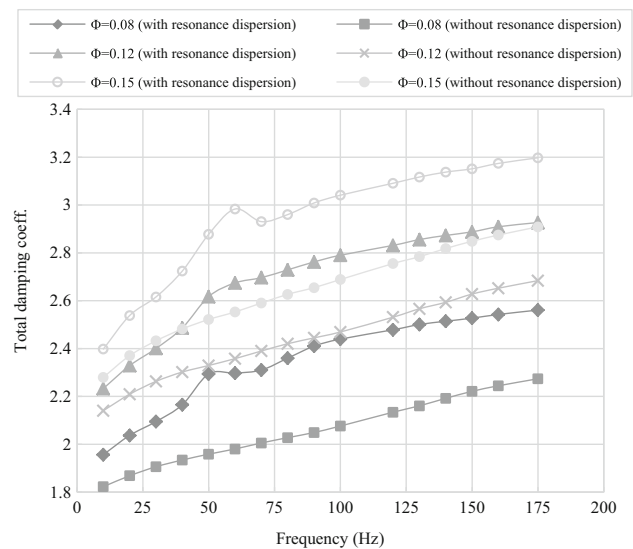


Fig. 11 Prediction of total damping coefficients for the acoustical system ($h_{rms} = 0.75$)

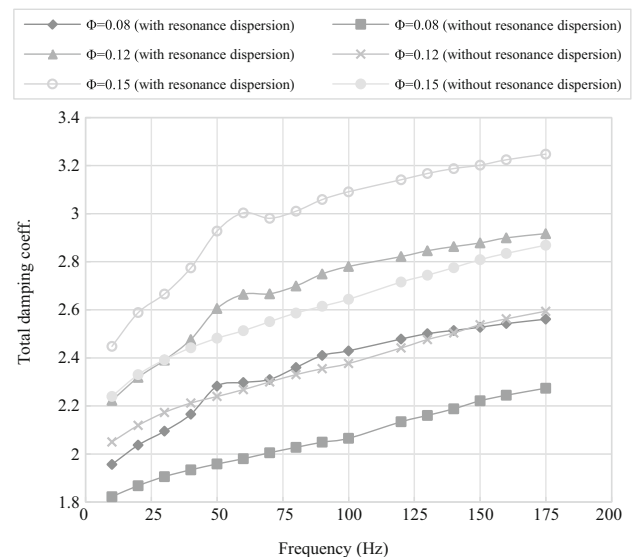


Fig. 12 Prediction of total damping coefficients for the acoustical system ($h_{rms} = 1.5$)

acoustical system when the frequency and the volume fraction increases.

As seen in Fig. 5, as volume fractions increase, the difference between the resulting damping coefficients from the RDM scheme and those of experimental tests grows. However, in the current study, volume fractions of 0.08, 0.12, and 0.15 are considered for which bubbles of radius 1 mm are distributed. As discussed by Medwin and Clay [18], the probability of the existence of bubbles of radius 1 mm in nature might not be too much. In fact, Medwin and Clay [18] mentioned that the dominant bubble radius generated from natural phenomena such as breaking waves

and wind blow is in the order of microns. In addition, as outlined by Medwin and Clay [18], it might be possible to study the marine environment by considering the dominant bubble radius and consequently calculate the resulting volume fraction. Therefore, the assumed volume fractions in this study, based on the dominant bubble radius, might be the most extreme cases for the bubble's population and volume fractions in reality, since the volume fraction in nature might be less than or at best equal to (in extreme cases) the ones considered here. Therefore, the error due to an increase in the volume fractions in the real conditions may not happen since the volume fractions are probably less than the ones considered here. However, as mentioned in the previous sections, some inexorable errors may occur in the final predicted results due to the assumptions such as considering a dominant bubble radius representing all bubbles of the bubbly medium. Nevertheless, through considering more realistic radii and distributions for bubbles, probable accumulation of errors might be addressed.

6 Conclusions

A new version of power-law attenuation is presented and applied to calculate the damping coefficients due to volumetric and scattering attenuation in an acoustical system which represents a real-sea condition. The acoustical system consists of water, bubbly water, and air media. To calculate the total damping inside the acoustical system, sound propagation within the system is divided into four different sequences and through the derived power-law attenuation relation, the attenuation relations for each sequence are derived, separately. The calculated damping coefficients resulting from the derived relations in each sequence are compared with Tolstoy's [6] results and reasonable agreement is achieved. In the resonance dispersion states, a peak is observed in the damping results at the frequency range of 50–60 Hz for all cases. In addition, when the interface of two media is smooth, the results of the resonance dispersion state are higher than those of non-resonance dispersion state at all frequencies. However, when the interface is rough, it is observed that below half of the natural frequency of the oscillation of bubbles, the results of resonance dispersion are higher than those of non-resonance dispersion state. Also, above half of the natural frequency range of the oscillation of bubbles, the results of non-resonance dispersion state are higher than the results of resonance dispersion state. Finally, after obtaining the damping coefficients of each sequence through the analogies of mechanical and acoustical systems, the total damping coefficient of the acoustical system is predicted at low frequencies in both resonance dispersion and non-resonance dispersion states. Results of total

damping coefficient vs. frequency at two different surface heights and three different volume fractions are presented. In the proposed modeling for the bubbly medium, a simplified model is considered in which bubbles of 1 mm radius are distributed in water and the vertical incident angle for the incident sound to the sea surface is taken into account. This can be considered as the first step before solving the very general problem of 3D spatial distribution of bubbles and wide distribution of sizes. Future work may also address more complicated conditions such as studying the influence of incident angles and propagation range on the attenuation of sound at sea surface.

Acknowledgements This research received no specific grant from any funding agency in the public, commercial, or not-for-profit sectors.

References

1. Grelowska G, Kozaczka E, Kozaczka S, Szymczak W (2013) Underwater noise generated by a small ship in the shallow sea. *Arch Acoust* 38:351–356
2. Godin OA (2007) Transmission of low-frequency sound through the water-to-air interface. *Acoust Phys* 53:305–312
3. Hayat T (2002) Scattering near a penetrable finite plane. *Arch Acoust* 27:41–53
4. Sikora M, Mateljan I, Bogunovic N (2012) Beam tracing with refraction. *Arch Acoust* 37:301–316
5. White MJ, Swenson Jr. GW, Borrowman TA, Borth JD (2011) Low-frequency sound propagation in porous media: glass spheres and pea gravel. Technical report, Department of Electrical and Computer Engineering, University of Illinois at Urbana-Champaign
6. Tolstoy I (1985) Rough surface boundary wave attenuation due to incoherent scatter. *J Acoust Soc Am* 77:482–488
7. Medwin H (1974) Acoustic fluctuations due to micro bubbles in the near-surface ocean. *J Acoust Soc Am* 56:1100–1104
8. Hall MV (1989) A comprehensive model of wind-generated bubbles in the ocean and predictions of the effects on sound propagation at frequencies up to 40 kHz. *J Acoust Soc Am* 86:1103–1117
9. McDonald BE (1991) Echoes from vertically striated subresonant bubble clouds: a model for ocean surface reverberation. *J Acoust Soc Am* 89:617–622
10. Henyey FS (1991) Acoustic scattering from ocean micro bubble plumes in the 100 Hz to 2 kHz region. *J Acoust Soc Am* 90:399–405
11. Prosperetti A, Lu NQ, Kim HS (1993) Active and passive acoustic behavior of bubble clouds at the ocean's surface. *J Acoust Soc Am* 93:3117–3127
12. Gauss RC, Fialkowski JM (1993) Measurements of the spectral characteristics of low-frequency, low-grazing-angles surface reverberation. *J Acoust Soc Am* 93:2299 (A)
13. Vereshchagina TN, Fedotovskiy VS, Derbenev AV, Prohorov YP (2006) Experimental research of resonance dispersion of low-frequency sound in gas-liquid media. Works of regional competition of science projects in natural sciences field, 9th edn. Kaluga Scientific Center, Kaluga, pp 86–99 (in Russian)
14. Godin OA (2006) Anomalous transparency of water-air interface for low frequency sound. *Phys Rev Letter* 97:164301
15. Godin OA (2008) Low-frequency sound transmission through a gas-liquid interface. *J Acoust Soc Am* 123:1862–1879

16. Godin OA (2008) Sound transmission through water-air interfaces: new insights into an old problem. *Contemp Phys* 49:105–123
17. Kuo EYT (1994) The perturbation characterization of reverberation from a wind-generated bubbly ocean surface—I: theory and a comparison of backscattering strength predictions with data. *IEEE J Ocean Eng* 19:368–381
18. Medwin H, Clay CS (1998) *Fundamentals of acoustical oceanography*, 2nd edn. Academic Press, Boston
19. Verestchagina TN, Fedotovskiy VS (2007) Low frequency resonance dispersion of sound in bubble media. XIX Session of the Russian Acoustical Society, pp 52–56
20. Klimonda Z, Litniewski J, Nowicki A (2011) Synthetic aperture technique applied to tissue attenuation imaging. *Arch Acoust* 36:927–935
21. Jensen FB, Kuperman WA, Porter MB, Schmidt H (2011) *Computational ocean acoustic*. Springer, New York
22. Szabo TL (1994) Time domain wave equations for lossy media obeying a frequency power law. *J Acoust Soc Am* 96:491–500
23. Szabo TL, Wu J (2000) A model for longitudinal and shear wave propagation in viscoelastic media. *J Acoust Soc Am* 107:2437–2446
24. Chen W, Holm S (2003) Modified Szabo's wave equation models for lossy media obeying frequency power law. *J Acoust Soc Am* 114:2570–2574
25. Brekhovskikh LM, Lysanov YuP (2003) *Fundamentals of Ocean Acoustics*. Press, Springer
26. Lamb H (1945) *Hydrodynamics*. Dover, New York
27. Minnaert M (1933) On musical air-bubbles and the sounds of running water. *Phil Mag* 16:235–248
28. Nakoryakov VE, Pokusaev BG, Shreiber IR (1983) *Propagation of waves in gas- and steam-liquid media*. Institute of thermophysics AS USSR, Novosibirsk (**in Russian**)
29. Skudzik E (1954) *Die Grundlagen der Akustik*. Springer, Wien